Nat. Hazards Earth Syst. Sci. Discuss., 1, 4425–4444, 2013
www.nat-hazards-earth-syst-sci-discuss.net/1/4425/2013/
doi:10.5194/nhessd-1-4425-2013

Natural Hazards and Earth System Sciences Discussions
Open Access

Spatial and temporal patterns of recent and future climate extremes in the Eastern Mediterranean and Middle East region

E. Kostopoulou[1], C. Giannakopoulos[2], M. Hatzaki[2], A. Karali[2], P. Hadjinicolaou[3], J. Lelieveld[3], and M. A. Lange[3]

[1]University of the Aegean, Department of Geography, Mytilene, Greece
[2]Institute for Environmental Research and Sustainable Development, National Observatory of Athens, Athens, Greece
[3]Energy, Environment and Water Research Center, The Cyprus Institute, Nicosia, Cyprus

Received: 2 August 2013 – Accepted: 11 August 2013 – Published: 4 September 2013

Correspondence to: E. Kostopoulou (ekostopoulou@aegean.gr)

Published by Copernicus Publications on behalf of the European Geosciences Union.

Abstract

Recent and future changes in temperature and precipitation climate extremes are estimated using the Hadley Centre PRECIS climate model for the Eastern Mediterranean and Middle East region. The area of interest is considered vulnerable to extreme climate events as there is evidence for a temperature rise while precipitation tends to decline, suggesting likely effects on vital socioeconomic sectors in the region. Observations have been obtained for the recent period (1961–1990) and used to evaluate the model output. The spatial distribution of recent temporal trends in temperature indicates strong increasing in minimum temperature over the eastern Balkan Peninsula, Turkey and the Arabian Peninsula. The rate of warming reaches 0.4–0.5 °C decade^{-1} in a large part of the domain, while warming is expected to be strongest in summer (0.6–0.7 °C decade^{-1}) in the E-Balkans and W-Turkey. The trends in annual and summer maximum temperature are estimated at approximately 0.5 and 0.6 °C decade^{-1}. Recent estimates do not indicate statistically significant trends in precipitation except for individual sub-regions. Results indicate a future warming trend for the study area over the last 30 yr of the 21st century. Trends are estimated to be positive and statistically significant in nearly the entire region. The annual trend patterns for both minimum and maximum temperature show warming rates of approximately 0.4–0.6 °C decade^{-1}, with pronounced warming over the Middle Eastern countries. Summer temperatures reveal a gradual warming (0.5–0.9 °C decade^{-1}) over much of the region. The model projects drying trends by 5–30 % in annual precipitation towards the end of the 21st century, with the number of wet days decreasing at the rate of 10–30 days yr^{-1}, while heavy precipitation is likely to decrease in the high-elevation areas by 15 days yr^{-1}.

NHESSD
1, 4425–4444, 2013

Spatial and temporal patterns of recent and future climate extremes

E. Kostopoulou et al.

1 Introduction

The last decades have seen a rapid growth in the development of regional climate models (RCMs) and the application of climate change projections to assess potential future effects of climate change on society, natural systems, and infrastructure on a regional scale. RCMs are widely utilized for simulation of regional and even local conditions (Rummukainen, 2010). Many studies emphasise on the assessment of their quality and usefulness to represent the natural climate variability (e.g. Vidale et al., 2003; Frei et al., 2006; Jacob et al., 2007; Christensen et al., 2007; Déqué et al., 2007; Kostopoulou et al., 2012), so that better projections of future climate change scenarios can be developed.

In this study, we use a regional climate model, based on the A1B scenario of the IPCC, to investigate climate changes in the Eastern Mediterranean and Middle East (EMME) regions, which seem to be particularly sensitive to climate change with pronounced warming and reduced precipitation (IPCC, 2007; Giorgi and Lionello, 2008; Sheffield and Wood, 2008). Arnell et al. (2004) showed that the countries most prone to increasing water stress are located around the Mediterranean and the Middle East. In the Middle East, climate change coupled with population growth is likely to reduce per capita water resources considerably, resulting in major social, economic, and environmental changes (Chenoweth et al., 2011). Previous research is relatively small for this part of the world due to data unavailability. The climate data restrictions result in local-scale studies which are limited to the use of point-data series. More studies can be found in the literature for the western part of our study region (Kostopoulou and Jones, 2005; Giannakopoulos et al., 2010; Hadjinicolaou et al., 2011). For instance, Kostopoulou and Jones (2005) studied possible changes in temperature and precipitation related climate extremes over the eastern Mediterranean region for the period 1958–2000. The most significant temperature trends were revealed for summer, where both minimum and maximum temperature extremes show statistically significant warming trends. Although, precipitation indices revealed regional contrasts, the eastern and

NHESSD
1, 4425–4444, 2013

southern stations indicated trends towards drier conditions. In a recent work, Unkašević and Tošić (2013) analysed extreme temperature indices at 15 stations in Serbia (for the period 1949–2009). They found that the climate conditions became warmer in the last 61 yr, and in agreement with Kostopoulou and Jones (2005) the most significant temperature trends were revealed for the summer season. Efthymiadis et al. (2011) used daily gridded datasets to detect trends in Mediterranean temperature extremes since the mid-20th century. The estimated trends were generally consistent with the global trends showing decrease in cold extremes and increase in warm/hot extremes. Zhang et al. (2005) examined trends in extreme temperature and precipitation indices at 52 stations from 15 countries in the Middle East region for the period 1950–2003. They found significant reductions in the number of cold days and increases in daily maximum and minimum temperature. Tayanç et al. (2009) showed a significant warming trend in southern and southeastern parts of Turkey for the period 1950–2004. Significant decreases in precipitation were found in the western parts of the country, although the variability of precipitation was substantially different across urban and rural areas, suggesting that urban stations can experience more frequent and severe droughts and floods. Fewer studies on changes in climate extremes can be found for areas further east, mainly due to the poor data network and limited access to long daily datasets required for such analyses. Recently, Almazroui et al. (2013) used daily observations from 27 stations from Saudi Arabia, with high-quality data for the period 1981–2010, to calculate climate indices and show that the temperature extremes in the region have significantly increased with larger rates in the recent-past (1996–2010) compared to a previous period (1981–1995).

RCM outputs help to overcome constraints associated with observational scarcity and are widely used for obtaining fine spatial and temporal resolution climate simulations for use in climate change impact studies. Within the framework of the CIMME project, the PRECIS RCM is run over the EMME region. The results of the project are summarised in a comprehensive regional climate assessment for the EMME region (Lelieveld et al., 2012). The study presented the natural climate variability during the past 500 yr based on natural proxies and documentary and analysed the climatology of the recent past. In addition, based on the output of the RCM the study introduced projections of climate change for the 21st century and summarised the potential impacts.

In this work, output from the PRECIS regional-scale climate model is further utilized and takes a step beyond the previous work done for the EMME domain. Our approach is to calculate trends for temperature and precipitation over the present and the future period to estimate current and predicted changes. We also calculate several extreme climate indices to detect signals of present and future changes. Future climate change is assessed by spatial patterns of change for selected extreme temperature and precipitation indices. The ultimate aim of the study is to identify regions in the study area that seem to undergo large amount of climate change, and provide information to policy-makers to develop management strategies for sectors which are likely to be impacted by the change, such as electricity demand, tourism and freshwater resources.

2 Data and methodology

2.1 Model data

The PRECIS ("Providing REgional Climates for Impacts Studies") climate model is an atmospheric and land surface model of limited area and high resolution (of 25 km), which is easily applicable over any part of the globe. Dynamical flow, the atmospheric sulphur cycle, clouds and precipitation, radiative processes, the land surface and the deep soil are all described. Boundary conditions are required at the limits of the model's domain to provide the meteorological forcing for the RCM (for a detailed description of the model see the PRECIS Handbook, Jones et al., 2004). The study uses daily temperature and precipitation projections from only one climate model, the Hadley Centre PRECIS regional climate model (driven by HadCM3P, Collins et al., 2005). This model output was preferred as it is run with a focus on the study region. The area of interest extends from 22° to 46° N and from

10° to 62° E, covering large portion of the EMME region. The model simulations were performed at the Cyprus Institute within the framework of the CIMME project (http://www.cyi.ac.cy/completed-research-projects-clima/item/201-cimme-climate-change-and-impacts-in-the-eastern-mediterranean-and-middle-east-project-completed.html), which studies "Climate Change and Impacts in the Eastern Mediterranean and Middle East".

The analysis of the present study focuses on two periods to describe present and future states of the climate for the study region. We use the classical 30-yr reference period of 1961–1990 to define the "present-day", whereas we define as "future" the time period from 2070–2099. Lelieveld et al. (2012) compared monthly CRU averages with PRECIS and showed that the model realistically reproduces climatic patterns and indices of extremes. In this study, the model results are evaluated against point observations available from 14 stations located at the NW part of the study area.

2.2 Methodological approach

First, we analyse the time series of daily minimum, maximum temperature and precipitation for the two time slices (present and future). The spatial patterns of the 30-yr mean conditions give a better indication of the gradients in temperature and precipitation patterns from the northern to the southern parts of the EMME region. We use linear models to identify temporal trends in the climatic variables over the 30-yr periods, which demonstrate local differentiations in the rates of change. According to the Fourth IPCC report (2007) "confidence has increased that some extremes will become more frequent, more widespread and/or more intense during the 21st century". To gain an insight in the perspective changes in climate extremes, we calculate several descriptive indices for temperature and precipitation extremes. Linear regression analysis was used to calculate trends in the indices and the patterns of modelled trends are presented and discussed.

NHESSD
1, 4425–4444, 2013

3 Results

3.1 Model evaluation

The daily bias is computed between model and station maximum (TX), minimum (TN) temperature and precipitation (RR). The 30-yr average bias for both TX, TN varies from −3.5 °C to 0 °C, indicating that the model has a cold bias, particularly observed at high altitudes. The correlation coefficients are 0.71–0.85 for TX and 0.68–0.82 for TN. The PRECIS daily precipitation does not correlate well with the observational data series ($r < 0.5$). The representation of temperature and precipitation annual cycles by PRECIS was examined for each station by calculating the mean value for each calendar-day over the reference period (Fig. 1). The averages for TX and TN are well represented for most stations, except for few model underestimations in winter TX, TN (e.g. Sarajevo, Bucharest) and overestimations in summer TX (e.g. Kneja, Beograd). These biases are confined to continental and high elevation stations and are possibly related to local effects (e.g. pronounced surface topography). The modelled annual precipitation cycles reproduce the observed wet/dry seasonal precipitation distribution in most cases, although model estimations of the mean daily precipitation are weak in general. In few sites the daily RR indicates a systematic underestimation of the model simulated summer precipitation in stations characterized by continental climates (e.g. Zagreb, Novo Mesto).

3.2 Model simulation of present-day climate

The mean climate conditions for the control period 1961–1990 over the study region confirm the known contrasting temperature and precipitation patterns between the northern and southern parts of the EMME region (Fig. 2). According to the model simulations, the annual mean temperature ranges from 0 °C in mountainous areas to 10–15 °C in most parts of the northern Mediterranean region. The southern part of the region, i.e. N-Africa and the Middle East, shows the warmer temperature pattern with averages in the range of 18–28 °C. Several sub-regions exhibit diverging distributions in precipitation, with annual totals ranging from over 1500 mm in the humid north (W-Balkans, NW-Turkey), to approximately 500 mm in Mediterranean lowlands (S-Balkans, W-Turkey) and to less than 200 mm in the arid south (Arabian Peninsula). Highly elevated areas receive large precipitation amounts indicating the predominant influence of orography on the spatial distribution of rainfall. The average patterns in relation to extreme temperature conditions are investigated based on the spatial distribution of winter TN and summer TX patterns. The winter average TN may reach as low as −10 °C in the mountainous areas and around 0 °C in continental parts north of 38 °N latitude. In S-Europe winter TN ranges from −5 to 10 °C, while further south it approximates 10 °C. The temperature contrasts between the northern and southern EMME sub-regions are particularly evident in the average summer TX, which ranges between 22–30 °C in the north, while further east and south it exceeds 40 °C.

In addition, annual and seasonal temperature and precipitation trends are assessed for the reference period. The 30-yr linear trend was determined for each grid point and the Kendall-tau test was employed to estimate the statistical significance of trends. Maps were constructed depicting only those grids with significant trends in TX and TN (Fig. 3). Strong positive trends in TN are found over the eastern Balkan Peninsula, Turkey and the Arabian Peninsula. The annual TN increases by 0.4–0.5 °C decade^{-1} in a large part of the domain, while during summer trends between 0.6–0.7 °C decade^{-1} are found in the E-Balkans and W-Turkey. The most prominent TN warming trends are seen in spring at a rate of about 0.7–0.8 °C decade^{-1}. The overall strongest warming over the reference period is found for spring TX reaching up to 0.9 °C decade^{-1} mainly occurred in the S-Balkans and Turkey. The trends in annual and summer TX are estimated at approximately 0.5 and 0.6 °C decade^{-1} especially in W-Turkey. The model results do not show an overall statistically significant trend in precipitation during the reference period, except for individual sub-regions, indicating decreases in the annual number of wet days and the amount of annual precipitation, mostly over Turkey (not shown).

NHESSD
1, 4425–4444, 2013

To assess extreme temperature and precipitation conditions in the EMME for the reference period (1961–1990) climate indices are calculated and expressed as the annual occurrence of a variable exceeding a certain threshold. The warming conditions are expressed by the number of "warm" days, which defines the annual count of days with TX > 25 °C, the number of "hot" days are defined as those with TX > 35 °C, and the number of tropical nights are days per year with TN > 20 °C. The number of frost nights are defined by days with TN < 0 °C. Regarding precipitation we use the average number of days (number of wet days) with RR > 1.0 mm, and heavy precipitation is defined by the annual number of days with RR > 10 mm.

The geographical patterns of the selected indices for the reference period, based on PRECIS output are presented in Fig. 4. Between the north and south of the EMME there can be a considerable difference in temperature, which is evident in the number of warm and hot days. The annual average number of days with TX exceeding 25 °C ranges from one month (in elevated areas) to three months in the northern EMME, while in the south two thirds of the year can be considered as warm days. Moreover, hot days occur at a maximum 30–50 days yr^{-1} in low elevation areas of the north and less than a month in areas of higher altitudes. In the southern EMME, days with temperature > 35 °C are common occurring up to five months per year (Gulf region). In contrast, continental (above 36° N) and high-altitude areas (across the Taurus and Zagros Mountains) experience up to 150 frost days yr^{-1}, while in the south the annual number of frost days does not exceed 20 days yr^{-1}. Further, tropical nights (TN > 25 °C) are rare (up to a month yr^{-1}) in the northern EMME, whereas in the south occur typically 1–2 months and more than 3 months yr^{-1} around the Persian Gulf. The north-south contrast becomes most evident from the precipitation indices patterns. Precipitation is typically heavier on the western slopes of the mountain ranges, while precipitation amounts decrease rapidly with latitude in the semi-arid southern EMME. The number of wet days (RR > 1 mm day^{-1}) during the reference period ranges from 200 days yr^{-1} in high altitudes and approximately 100 days yr^{-1} in the northern parts, to less than 40 days yr^{-1} in the southern parts. Along the western edge of the Balkan Peninsula

NHESSD
1, 4425–4444, 2013

and other high-elevation areas (e.g. Caucasus), heavy precipitation occurs during maximum 50 days yr^{-1}. The same occurs for about 30–40 days yr^{-1} over the Taurus mountain range in S-Turkey, and the Zagros Mountains, which extend along southern and western Iran into northern Iraq. Over the reference period, the occurrence of heavy precipitation days is unusual in the southern EMME region.

3.3 Projected temperature and precipitation changes

In the following, we discuss the mean climate change for 2070–2099 and Fig. 5 provides key insights in the projected temperature change, presenting the distribution of statistically significant trends in annual, spring and summer TX and TN. Trends are estimated to be positive in all cases and statistically significant in nearly the entire study region. The annual trend patterns for both TN, TX show similar warming rates of approximately 0.4–0.6 °C $decade^{-1}$. Consistent with the findings for the reference period, the model projections suggest prominent trends in spring TN and TX, which increases by 0.6–0.8 and 0.7–0.9 °C $decade^{-1}$, respectively, with pronounced warming over the Middle Eastern countries. Summer temperatures reveal a gradual warming (0.5–0.9 °C $decade^{-1}$) over much of the region. For precipitation only few grids were found to present statistically trends, and therefore their patterns are not discussed.

We defined the "present-day" period as 1961–1990 and "future" as the time period from 2070–2099, and computed differences in climate indices between these two periods (Fig. 6). The number of warm days is found to increase in particular in the northern part of EMME by 50–60 additional days per year by the end of the 21st century. Hot days are estimated to occur much more frequently in the EMME. In particular, low-elevation and coastal regions in the northern part are estimated to experience about 1–2 extra months with $TX > 35$ °C, while the warmer and arid southern parts are expected to face conditions with two additional months of hot days per year. It is estimated that the warmer future of the area will also include strong increases in the occurrence of warm nights. The change in the number of tropical nights translates to 1–2 additional months of tropical nights per year in the north and to 3 additional months in the

NHESSD
1, 4425–4444, 2013

southern EMME by the end of the 21st century. Towards a warmer future climate in EMME, the number of frost days is found to decline within a range of 1–2 months of fewer frost days yr^{-1} (in high-latitude continental and high-altitude locations). Regarding precipitation, PRECIS shows that in the northern EMME, the number of wet days may decrease by 10–30 days yr^{-1}, while heavy precipitation is likely to decrease in the high-elevation areas by 15 days yr^{-1} by the end of the 21st century.

4 Conclusions

Utilising output from the Hadley Centre PRECIS climate model, we studied the spatial distribution and temporal trends in temperature and precipitation and their extremes in the Eastern Mediterranean and Middle East region. The calculated trends indicate statistically significant warming over land in the EMME of approximately 0.5–0.6 °C decade^{-1}, which is projected to continue into the future. The warming trends are found in annual and seasonal daily TX and TN, with the spring temperatures increasing at a faster rate. Towards a warmer and drier climate in EMME the PRECIS results suggest increases of warm, hot days, and tropical nights. The projected increase of TX is most rapid in the northern EMME, by up to two months of additional warm days per year by the end of the 21st century. In contrast, frost days and wet days are projected to decrease. The trends in present and future precipitation, based on the model data, were more uncertain, however the future precipitation indices showed decrease in the number of wet days and the heavy precipitation events towards the end of the 21st century. The combination of long-term changes and the greater frequency of extreme climate events can have adverse impacts on many economic sectors in EMME while excessive heat stress and reduced water resources will have important negative consequences for human health and ecosystems.

Acknowledgements. We thank the CIMME project team for the regional climate assessment (Climate change and Impacts in the Eastern Mediterranean and Middle East) and the Hadley Centre (UK) for providing the PRECIS model.

References

Almazroui, M., Nazrul Islam, M., Dambul, R., and Jones, P. D.: Trends of temperature extremes in Saudi Arabia, Int. J. Climatol., online first, doi:10.1002/joc.3722, 2013.

Arnell, N. W.: Climate change and global water resources: SRES emissions and socio economic scenarios, Global Environ. Change, 14, 31–52, 2004.

Collins, M., Booth, B. B. B., Harris, G. R., Murphy, J. M., Sexton, D. M. H., and Webb, M. J.: Towards quantifying uncertainty in transient climate change, Clim. Dynam., 27, 127–147, 2005.

Chenoweth, J., Hadjinicolaou, P., Bruggeman, A., Lelieveld, J., Levin, Z., Lange, M. A., Xoplaki, E., and Hadjikakou, M.: The impact of climate change on the water resources of the eastern Mediterranean and Middle East region: modelled 21st century changes and implications, Water. Resour. Res., 47, W06506, doi:10.1029/2010WR010269, 2011.

Christensen, J. H., Carter, T. R., Rummukainen, M., and Amanatidis, G.: Evaluating the performance and utility of regional climate models: the PRUDENCE project, Climatic Change, 81, 1–6, 2007.

Déqué, M., Rowell, D. P., Lüthi, D., Giorgi, F., Christensen, J. H. , Rockel, B., Jacob, D., Kjellström, E., de Castro, M., and van den Hurk, B.: An intercomparison of regional climate simulations for Europe: assessing uncertainties in model projections, Climatic Change, 81, 53–70, 2007.

Efthymiadis, D., Goodess, C. M., and Jones, P. D.: Trends in Mediterranean gridded temperature extremes and large-scale circulation influences, Nat. Hazards Earth Syst. Sci., 11, 2199–2214, doi:10.5194/nhess-11-2199-2011, 2011.

Frei, C., Schöll, R., Fukutome, S., Schmidli, J., and Vidale, P. L.: Future change of precipitation extremes in Europe: Intercomparison of scenarios from regional climate models, J. Geophys. Res. Atmos., 111, D06105, doi:10.1029/2005JD005965, 2006.

Giannakopoulos, C., Hadjinicolaou, P., Kostopoulou, E., Varotsos, K. V., and Zerefos, C.: Precipitation and temperature regime over Cyprus as a result of global climate change, Adv. Geosci., 23, 17–24, doi:10.5194/adgeo-23-17-2010, 2010.

Giorgi, F. and Lionello, P.: Climate change projections for the Mediterranean region, Global Planet. Change, 63, 90–104, 2008.

NHESSD

1, 4425–4444, 2013

Spatial and temporal patterns of recent and future climate extremes

E. Kostopoulou et al.

Hadjinicolaou, P., Giannakopoulos, C., Zerefos, C., Lange, M. A., Pashiardis, S., and Lelieveld, J.: Mid-21st century climate and weather extremes in Cyprus as projected by six regional climate models, Reg. Environ. Change, 11, 441–457, 2011.

IPCC: The Physical Science Basis, in: Contribution of Working Group I to the Fourth Assessment Report of the Intergovernmental Panel on Climate Change, edited by: Solomon, S., Qin, D., Manning, M., Chen, Z., Marquis, M., Averyt, K. B., Tignor, M., and Miller, H. L., Cambridge University Press, Cambridge, United Kingdom and New York, NY, USA, 996 pp., 2007.

Jacob, D., Bärring, L., Christensen, O. B., Christensen, J. H., de Castro, M., Déqué, M., Giorgi, F., Hagemann, S., Hirschi, M., Jones, R., Kjellström, E., Lenderink, G., Rockel, B., Sánchez, E., Schär, C., Seneviratne, S., Somot, S., van Ulden, A., and van den Hurk, B.: An intercomparison of regional climate models for Europe: model performance in present-day climate, Climatic Change, 81, 31–52, 2007.

Jones, R. G., Noguer, M., Hassell, D. C., Hudson, D., Wilson, S. S., Jenkins, G. J., and Mitchell, J. F. B.: Generating high resolution climate change scenarios using PRECIS, Met Office Hadley Centre, Exeter, UK, 40 pp., 2004.

Kostopoulou, E. and Jones, P. D.: Assessment of climate extremes in the Eastern Mediterranean, Meteorol. Atmos. Phys., 89, 69–85, 2005.

Kostopoulou, E., Giannakopoulos, C., Hatzaki, M., and Tziotziou, K.: Climate extremes in the NE Mediterranean: assessing the E-OBS dataset and regional climate simulations, Clim. Res., 54, 249–270, 2012.

Lelieveld, J., Hadjinicolaou, P., Kostopoulou, E., Chenoweth, J., Giannakopoulos, C., Hannides, C., Lange, M. A., El Maayar, M., Tanarhte, M., Tyrlis, E., and Xoplaki, E.: Climate change and impacts in the Eastern Mediterranean and the Middle East, Climatic Change, 114, 667–687, 2012.

Rummukainen, M.: State-of-the-art with regional climate models, WIREs Clim. Change, 1, 82–96, 2010.

Sheffield, J. and Wood, E. F.: Projected changes in drought occurrence under future global warming from multi-model, multi scenario, IPCC AR4 simulations, Clim. Dynam., 31, 79–105, 2008.

Tayanç, M., İm, U., Doğruel, M., and Karaca M.: Climate change in Turkey for the last half century, Climatic Change, 94, 483–502, 2009.

Unkašević, M. and Tošić, I.: Trends in temperature indices over Serbia: relationships to large-scale circulation patterns, Int. J. Climatol., online first, doi:10.1002/joc.3652, 2013.
Vidale, P. L., Lüthi, D., Frei, C., Seneviratne, S. I., and Schär, C.: Predictability and uncertainty in a regional climate model, J. Geophys. Res., 108, 4586, doi:10.1029/2002JD002810, 2003.
Zhang, X., Aguilar, E., Sensoy, S., Melkonyan, H., Tagiyeva, U., Ahmed, N., Kutaladze, N., Rahimzadeh, F., Taghipour, A., Hantosh, T. H., Albert, P., Semawi, M., Ali, M. K., Al-Shabibi, M. H. S., Al-Oulan, Z., Zatari, T., Al Dean Khelet, I., Hamoud, S., Sagir, R., Demircan, M., Eken, M., Adiguzel, M., Alexander, L., Peterson, T. C., and Wallis, T.: Trends in Middle East climate extreme indices from 1950 to 2003, J. Geophys. Res.. 110, D22104, doi:10.1029/2005JD006181, 2005.

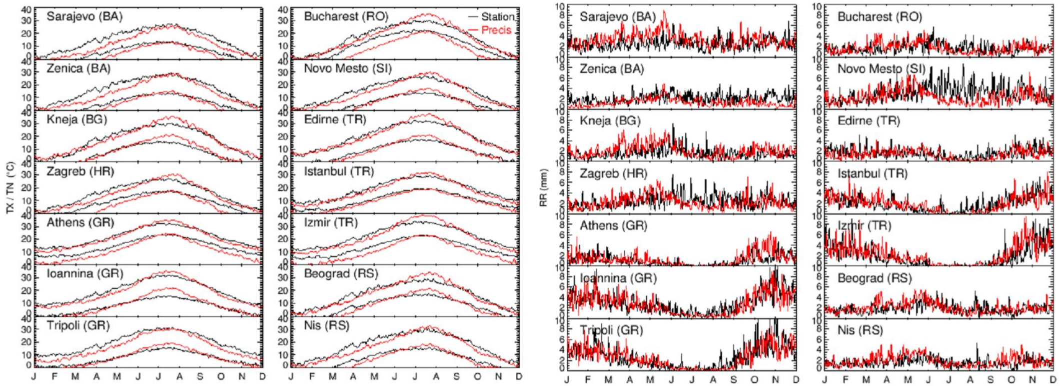

Fig. 1. Temperature (left) and precipitation (right) annual cycle of 14 examined stations as represented by station (black line) and model (red line) data. In temperature diagrams, the upper (lower) pair of lines represents maximum (minimum) temperature.

NHESSD
1, 4425–4444, 2013

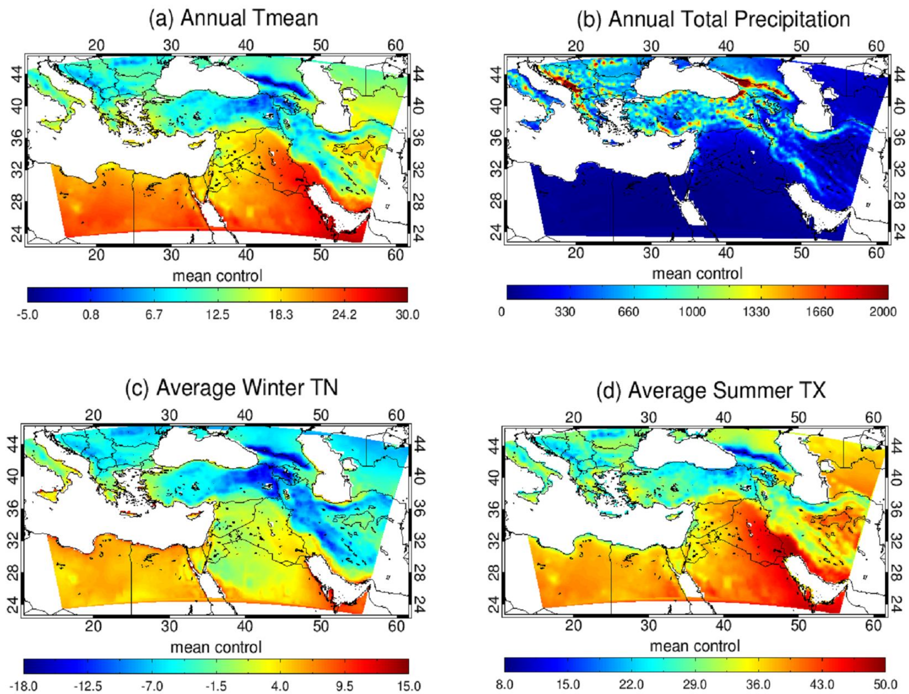

Fig. 2. Average annual mean temperature **(a)**, total annual precipitation **(b)**, average winter minimum temperature **(c)** and average summer maximum temperature **(d)** based on the model control runs for the reference period 1961–1990.

NHESSD
1, 4425–4444, 2013

Spatial and temporal patterns of recent and future climate extremes

E. Kostopoulou et al.

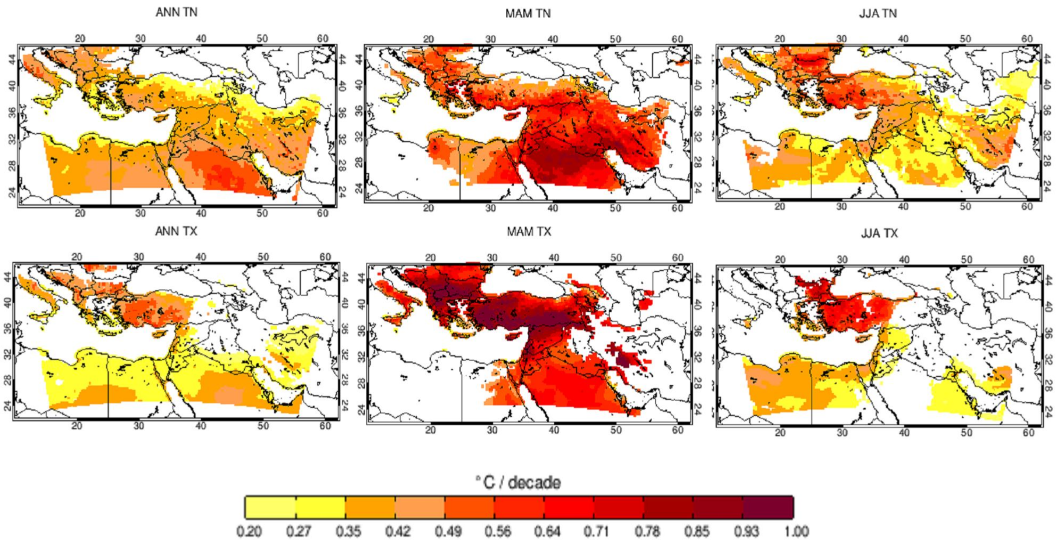

Fig. 3. Annual (left column), spring (middle column) and summer (right column) statistically significant trends for minimum (TN) and maximum (TX) temperatures (top, bottom row respectively) over the period 1961–1990.

NHESSD
1, 4425–4444, 2013
Spatial and temporal patterns of recent and future climate extremes
E. Kostopoulou et al.

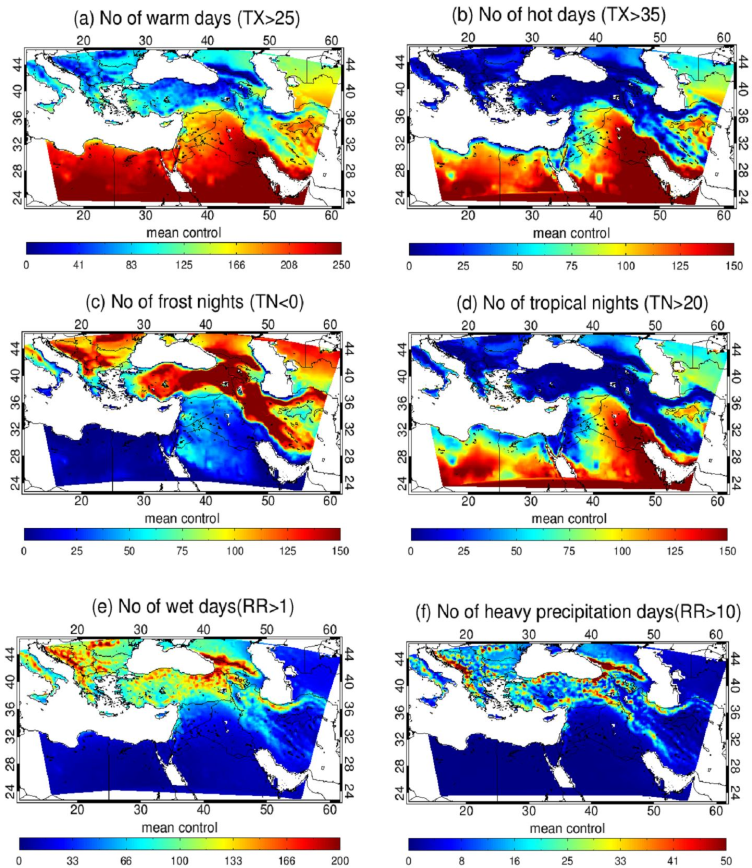

Fig. 4. Patterns of temperature and precipitation indices showing the mean number of days per year during the control period 1961–1990.

NHESSD
1, 4425–4444, 2013

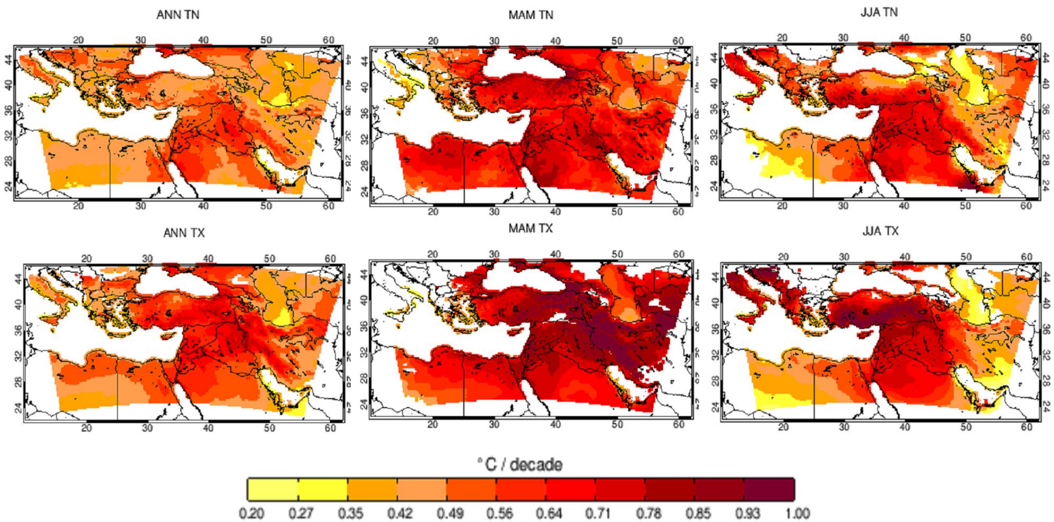

Fig. 5. As in Fig. 3 for the future period 2070–2099.

NHESSD
1, 4425–4444, 2013

Spatial and temporal patterns of recent and future climate extremes

E. Kostopoulou et al.

Title Page
Abstract | Introduction
Conclusions | References
Tables | Figures
◀| |▶
◀ ▶
Back | Close
Full Screen / Esc
Printer-friendly Version
Interactive Discussion

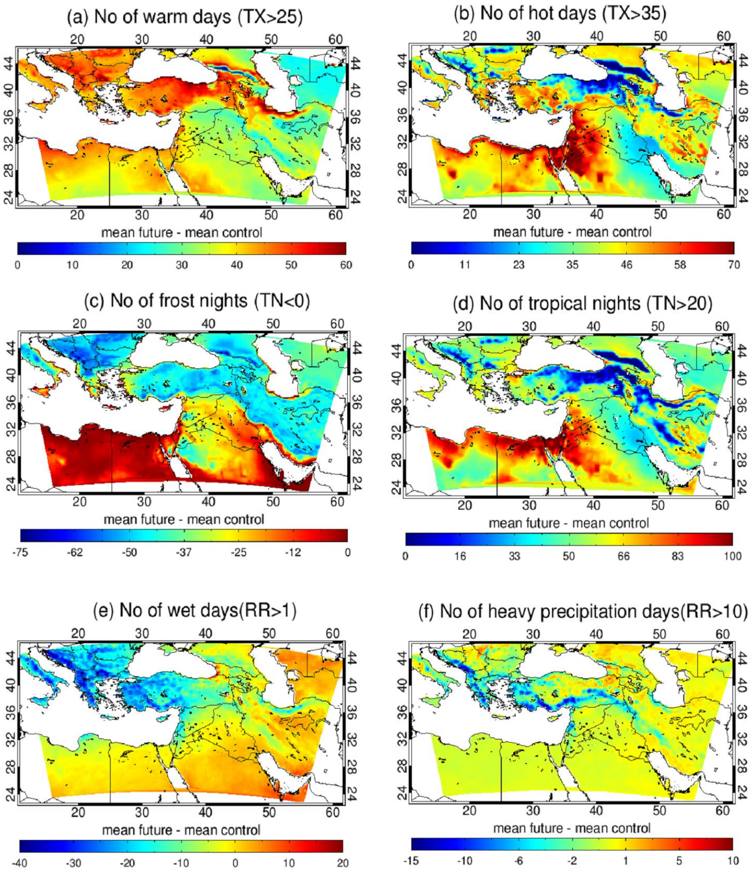

Fig. 6. Patterns showing the mean changes in temperature and precipitation indices for the future period 2070–2099 relative to the control period 1961–1990.

NHESSD
1, 4425–4444, 2013